International Journal of Applied Science and Engineering

Comparative analysis of GaAs solar cells performance using different FSF and BSF material sets

Ala'eddin A. Saif *

Physics Department, College of Science, University of Jeddah, Jeddah, Saudi Arabia

ABSTRACT

This study aims to analyze the impact of varying the front surface field (FSF) and back surface field (BSF) materials using $Al_{0.8}Ga_{0.2}As$, $(Al_{0.7}Ga_{0.3})_{0.5}In_{0.5}P$, and $In_{0.49}Ga_{0.51}P$ in pairs on single-junction GaAs solar cells performance with the aid of the SILVACO simulator. The solar cells with different FSF and BSF material sets are compared based on the photogeneration, recombination, and energy band structure. The results show that the initial cell without FSF and BSF gives an efficiency of 11.42%. When AlGaAs is used as the FSF layer the efficiency is significantly enhanced to 25.65%, 25.72%, and 30.16% as AlGaAs, InGaP, and AlGaInP are used for the BSF layer, respectively. When InGaP is utilized as the FSF layer, the efficiency also increases to 24.05%, 24.12%, and 27.94% as AlGaAs, InGaP, and AlGaInP are served as the BSF layer, respectively. The efficiency enhancement when AlGaAs and InGaP are used as the FSF is correlated to their high energy bandgap that enhances the photogeneration rate and smoothens the flow of photogenerated electrons toward the back contact. The extreme performance of the cells with AlGaInP BSF is attributed to the high potential barrier for the valance band between the base and BSF layer, which enhances the ability to confine the photogenerated holes in the solar cell and smoothen their flow toward the front contact. While using AlGaInP as the FSF layer, the cells' efficiency is degraded to about 6% regardless of the BSF material, which is due to the high potential barrier height for the conduction band between FSF and emitter and the low potential step between the emitter and base leading to a higher recombination rate for photogenerated electrons within the emitter. Based on this study, the best FSF and BSF materials set to obtain an optimum GaAs solar cell performance are AlGaAs and AlGaInP, respectively.

Keywords: Energy band diagram, GaAs solar cell, Photogeneration, Recombination, SILVACO

OPEN ACCESS

Received: May12, 2024
Revised: May 30, 2024
Accepted: July 20, 2025

Corresponding Author:
Ala'eddin A. Saif
aasaif@uj.edu.sa

Publisher:
Chaoyang University of Technology
ISSN: 1727-2394 (Print)
ISSN: 1727-7841 (Online)

1. INTRODUCTION

With the global increasing demand for energy, scientists are working hard on generating electric energy based on clean and sustainable solar energy instead of using traditional resources such as oil and coal due to their environmental issues (Singh and Verma, 2018; Abu-Shamleh et al., 2021). Since discovering the photovoltaic effect, researchers suggested many materials to act as the active material for solar cells to obtain the maximum possible efficiency. Among these materials, gallium arsenide (GaAs) receives high attention due to its outstanding photo-absorption coefficient and high mobility, besides its reasonable direct energy bandgap of 1.42 eV that matches most solar spectrum photons energy, which guarantees the maximum absorption ability for the solar cells (Aissat et al., 2017; Singh et al., 2022).

The absorption ability of GaAs solar cells for shorter wavelengths can be improved by inserting a wider bandgap material as a top window layer, or what so-called front surface field (FSF) layer, that works also on minimizing the recombination for the photogenerated carriers at the top surface of the cell (Bourbaba et al., 2019). Moreover,

GaAs solar cells also suffer from recombination for the carriers at the bottom surface of the cell, this issue can be minimized by introducing another layer of higher energy bandgap at the back side of the cell called the back surface field (BSF) (Arzbin and Ghadimi, 2019), which also acts to confine the photogenerated carriers, which in turn increases the photogenerated current (Islam et al., 2011). Thus, using FSF and BSF layers together to fabricate GaAs solar cells would enhance the cell performance, particularly, its efficiency.

Researchers have proposed many materials such as InGaP, InAlP, AlGaAs, and InAlGaP to be used as FSF or BSF layers, where most of the reports in the literature focused on using AlGaAs as BSF layers. For instance, a study by Palacios et al. (2018) suggested a homojunction GaAs with AlGaAs as FSF and BSF gives an efficiency of ~24.5%. Another study reported by Attari et al. (2017) suggested using InAlGaP as FSF and AlGaAs as BSF for a single junction GaAs solar cell with the aid of the genetic algorithm method to predict the optimum doping and thickness of cell layers, which records an efficiency of 29.7%. Gamel et al. (2019) presented a GaAs solar cell with InAlP as FSF and AlGaAs as BSF, which it is tested in the presence of 1-sun and 100-sun AM 1.5 spectrum to obtain 24.08% and 27.22% efficiency, respectively. In previous works by our team, a GaAs solar cell with InAlP as FSF and InAlGaP as BSF is proposed and it shows an efficiency of 30.88% (Saif, 2023).

Selecting the materials for FSF and BSF layers is a very critical step in fabricating an efficient GaAs solar cell. Their lattice should be matched with the active regions to ensure minimum charge traps at the interfaces since they increase the recombination rate at the interfaces (Gamel et al., 2019). In addition, the FSF layer should exhibit a wider bandgap than GaAs to enable higher energy photon absorption. The same condition is applied on the BSF layer to offer higher confinement for the photogenerated carriers within the cell. Further understanding of the influence of the energy band structure of the FSF and BSF layers needs further investigation. In this work, three materials, namely: $Al_{0.8}Ga_{0.2}As$, $(Al_{0.7}Ga_{0.3})_{0.5}In_{0.5}P$, and $In_{0.49}Ga_{0.51}P$, have been suggested to act as FSF layer and/or BSF layer for the GaAs solar cells. This research aims to analyze and compare the performance of the GaAs solar cells that are constructed of these materials in pairs as FSF and BSF layers at fixed doping concentration and thickness for cells' regions, then correlate their efficiency values with the energy band structure to find out the best material combination to serve as FSF and BSF layers.

2. MATERIALS AND METHODS

An initial single junction GaAs solar cell is architected as shown in Fig. 1(a). Then, FSF and BSF layers are introduced by varying their materials using $Al_{0.8}Ga_{0.2}As$, $(Al_{0.7}Ga_{0.3})_{0.5}In_{0.5}P$, and $In_{0.49}Ga_{0.51}P$, as shown in Fig. 1(b). Thus, one of these materials is assigned as the FSF layer, and the BSF layer is varied with the three materials. For all cases, the FSF layer is p-type doped and BSF is n-type doped.

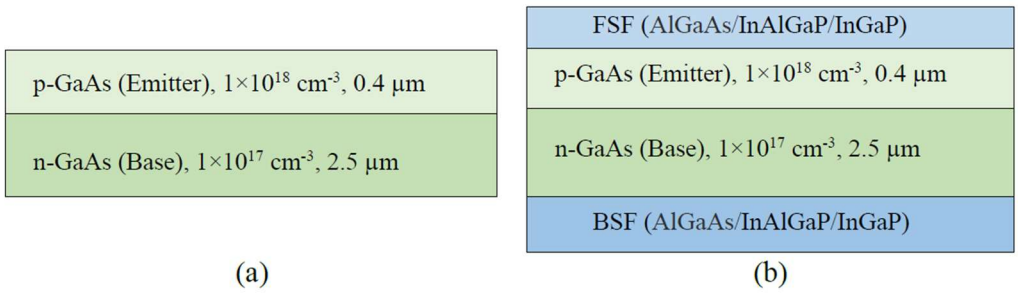

Fig. 1. The construction of (a) initial GaAs cell and (b) with FSF and BSF layers

Table 1. Material parameters used in solar cell simulation (Saif, 2023; Saif et al., 2023)

Parameter	*GaAs*	*$In_{0.49}Ga_{0.51}P$*	*$Al_{0.8}Ga_{0.2}As$*	*$(Al_{0.7}Ga_{0.3})_{0.5}In_{0.5}P$*
Lattice constant (Å)	5.65	5.65	6.65	5.65
Energy bandgap (eV)	1.42	1.9	2.09	2.4
Permittivity	13.2	11.62	11.7	11.7
Affinity (eV)	4.07	4.16	3.53	4.2
e- mobility MUN (cm^2/Vs)	8800	1945	212.2	2150
h+ mobility MUP (cm^2/Vs)	400	141	67.6	141
e- density of states NC300 (cm^{-3})	4.35×10^{17}	1.3×10^{20}	1.58×10^{19}	1.2×10^{20}
h+ density of states NV300 (cm^{-3})	1.29×10^{19}	1.28×10^{19}	1.5×10^{19}	1.28×10^{19}

Lifetime (electrons) TAUN (s)	1×10^{-9}	1×10^{-9}	1×10^{-9}	1×10^{-9}
Lifetime (holes) TAUP (s)	2×10^{-8}	1×10^{-9}	2×10^{-8}	1×10^{-9}

These cells are architected using SILVACO TCAD by setting the physical parameters of the material that are summarized in Table 1 (Saif, 2023; Saif et al., 2023). The thickness and doping level of the FSF are 0.05 µm and 3 $\times 10^{18}$ cm^{-3}, respectively, and of the BSF layer are 1.0 µm and 1 $\times$ 10^{20} cm^{-3}, respectively. The solar cells are tested under illumination to the AM 1.5G spectrum to ensure the collection of all the solar wavelengths.

3. RESULTS AND DISCUSSION

3.1 Initial Cell Characteristics

The extracted photogenerated current density vs anode voltage (J-V) curve of the initial solar cell is represented in Fig. 2. From the curve, the calculated electrical parameters short circuit current density (J_{sc}), open circuit voltage (V_{oc}), maximum power (P_{max}), fill factor (FF), and conversion efficiency (η) are 14.64 mA/cm^2, 0.91 V, 11.4 mW/cm^2, 85.76%, and 11.42%, respectively.

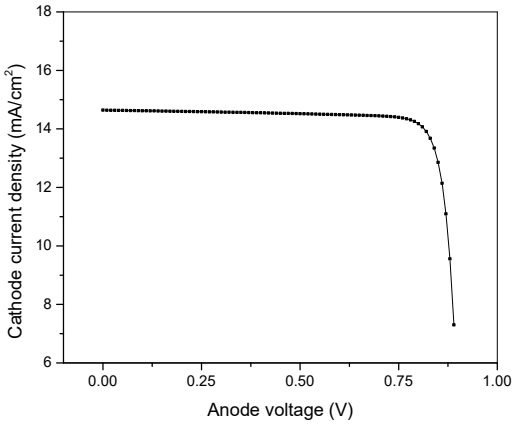

Fig. 2. J-V curve for the initial GaAs solar cell

For further understanding of the tested GaAs solar cell, a cross-section of the photogeneration rate and recombination rate as a function of cell thickness from the top is plotted in Fig. 3. It can be observed from Fig. 3(a) that the photogeneration rate of carriers through the emitter decreases from its maximum value of 22.08 $cm^{-3}{\cdot}s^{-1}$ to 21.21 $cm^{-3}{\cdot}s^{-1}$ and then continues decreasing through the base region to its minimum value of 19.84 $cm^{-3}{\cdot}s^{-1}$. The recombination rate in Fig. 3(b) is minimal at the edges of the cell and the PN depletion region of the cell, and it peaks within the emitter and base regions. It is found that the ratio of the photogenerated rate to the average recombination rate at the emitter and base layers is of order 3.97 $\times$ 10^3 and 14.3, respectively. This means that most of the recombination for carriers occurs within the base region.

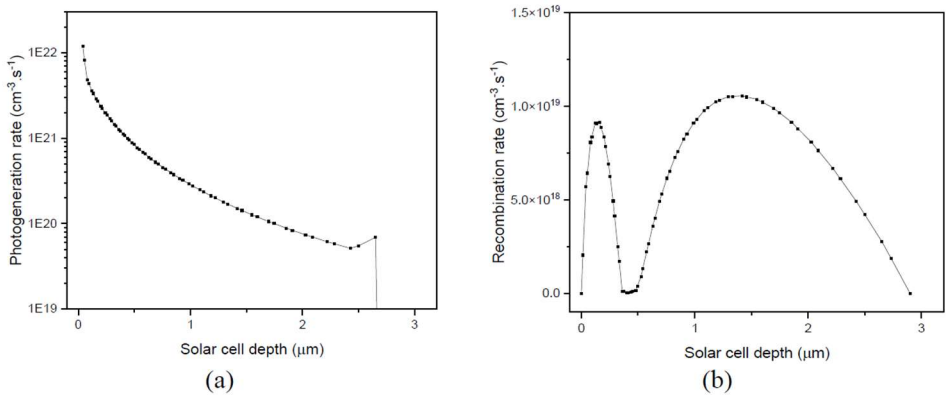

Fig. 3. A cross-section view along the initial solar cell for (a) photogeneration rate and (b) recombination rate

3.2 Using AlGaAs as FSF Layer

The J-V characteristics for GaAs solar cells that are constructed with p-AlGaAs to act as the FSF layer and n-AlGaAs, n-AlGaInP, and n-InGaP as the BSF layer are shown in Fig. 4. The obtained cells' parameters are summarized in Table 2. From the results, it is found that the cells that exhibit AlGaAs and InGaP as BSF layers show almost identical J-V curves and very close parameters. Comparably, the conversion efficiency of the cells with FSF and BSF layers is remarkably improved. Further, one can conclude that the cell that is structured with AlGaInP as the BSF layer shows notably higher conversion efficiency as compared to the other cells with AlGaAs or GaInP as the BSF layer. The obtained η value of the solar cells in this work with AlGaAs as FSF layer is comparable with the one reported in the literature regardless of the material used for the BSF layer (Zhao et al., 2016; Palacios et al., 2018; Gamel et al., 2019; Kamdem et al., 2019).

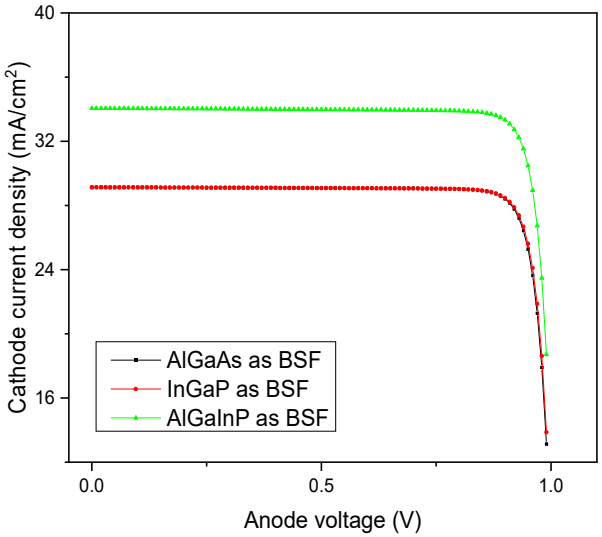

Fig. 4. J-V characteristics for GaAs solar cells with AlGaAs as FSF and different BSF materials

Table 2. Parameters of GaAs solar cells with AlGaAs as FSF and different BSF materials

Parameter	*AlGaAs as BSF*	*InGaP as BSF*	*AlGaInP as BSF*
J_{sc} (mA/cm^2)	29.14	29.13	34.06
V_{oc} (V)	1.007	1.007	1.010
P_{max} (mW/cm^2)	25.61	25.69	30.12
FF (%)	87.30	87.58	87.49
η (%)	25.65	25.72	30.16

To explain the behavior of these cells, a cross-section of the photogeneration and recombination rates along the cell thickness is plotted in Fig. 5. It can be noticed that all cells show similar attitudes through the top layers, the difference appears due to varying the BSF layer material. Generally, it can be seen that the photogeneration rate for all cells shows a maximum value of 5.12×10^{21} cm^{-3}·s^{-1} at the top surface of FSF then decreases through it until 1.72×10^{21} cm^{-3}·s^{-1}, then it is maximized again at the emitter interface to a value of the 1.12×10^{22} cm^{-3}·s^{-1} and reduces through it up to a value of 1.86×10^{21} cm^{-3}·s^{-1}, then continue decreasing through the base to its minimum value of 1.83×10^{19} cm^{-3}·s^{-1} as illustrated in Fig. 5(a). Within BSF, the cells that are made by AlGaAs and InGaP show a further decrement in photogeneration rate in the BSF layer. The cell that is constructed with AlGaInP as the BSF layer displays an abrupt increase in photogeneration rate to a new maximum value and weakly decreases through it. This increment in photogeneration rate indicates that AlGaInP has a high capability to confine extra photogenerated carriers through the cell, which explains the high efficiency of this cell as compared to the cells with AlGaAs and InGaP BSF layers.

Fig. 5(b) depicts the recombination rate through these cells. It can be observed that the carrier recombination rate within FSF is minimal, which confirms the role of this layer. Then it increases and crests within the emitter, and then it minimizes within the GaAs p-n junction after that slightly increases inside the base region. The strong recombination rate within the emitter could be due to the relatively high photogeneration rate of the carriers within the emitter. For the cells consisting of AlGaAs and InGaP as the BSF layer, the recombination rate drops to a minimal value, while in the cell with AlGaInP as the BSF layer, it incredibly increases forming a crest within the AlGaInP layer, which could be due to the high photogeneration rates within this layer, as seen in Fig. 5(a). The slightly high recombination within the base layer for all cells is due to the presence of the BSF layer that works on increasing the confinement of carriers within the base region, thus more probability for them to get recombined within the base. Furthermore, it is found that the photogeneration to recombination ratios within the AlGaAs, InGaP, and AlGaInP BSF layers are 1.003, 3.440, and 8.270, respectively. Indicating that the cell with the AlGaInP layer has the highest number of photogenerated carriers that are successfully collected on contacts before they are recombined (Ansari et al., 2019), which explains the comparably high conversion efficiency of this cell over the other cells.

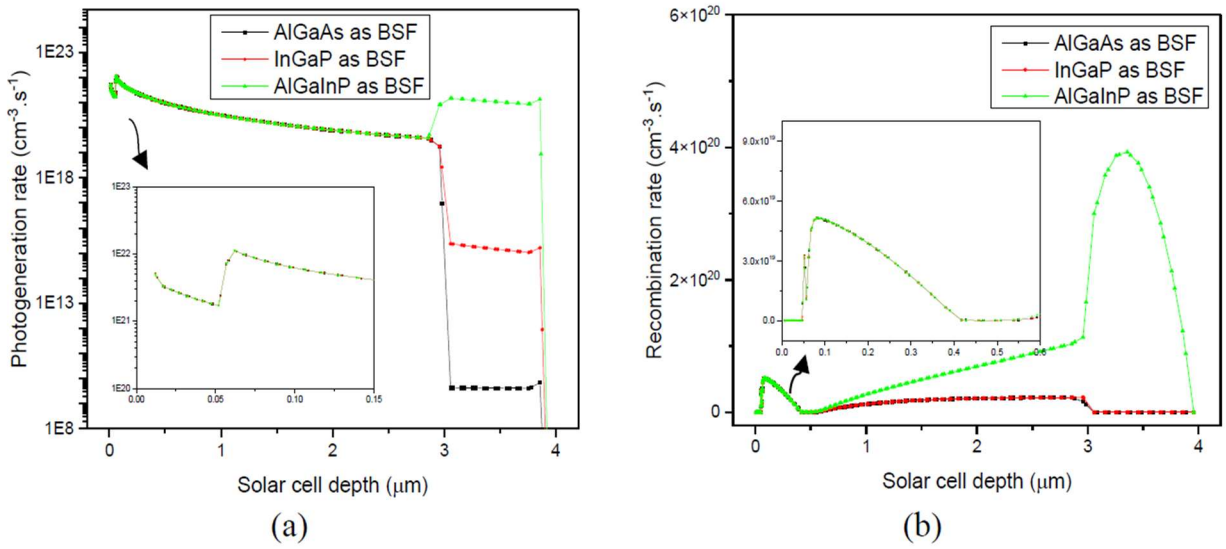

Fig. 5. A cross-section of the (a) photogeneration rate and (b) recombination rate of GaAs solar cells with AlGaAs as FSF and different BSF materials

3.3 Using InGaP as FSF Layer

Fig. 6 illustrates the J-V characteristics for GaAs solar cells constructed with p-InGaP as FSF layers and n-AlGaAs, n-AlGaInP, and n-InGaP as BSF layers separately. The cells' parameters are tabulated in Table 3. From the results, it can be noticed that the cells that have AlGaAs and InGaP as BSF layer show similar J-V curves and almost identical cell parameters, except for the cell with InGaP shows a slightly higher fill factor and efficiency. However, the cell that is configured with AlGaInP as the BSF layer shows notably higher short circuit current density, maximum power, and conversion efficiency as compared to the other cells. Generally, the obtained η values of the current cells with InGaP FSF layer is comparable with the values reported in the previous studies (Xu et al., 2017; Devendra et al., 2020).

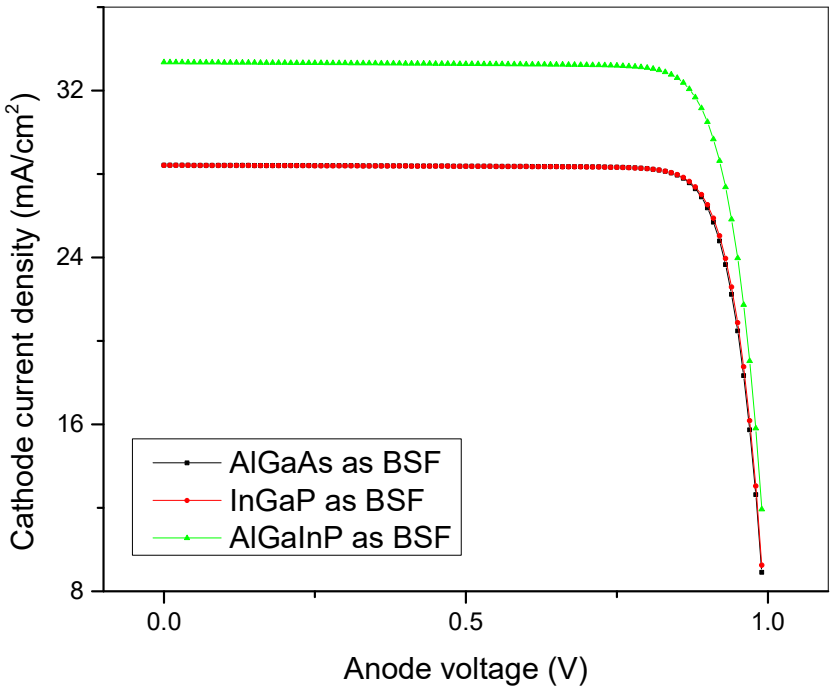

Fig. 6. J-V characteristics for GaAs solar cells with InGaP as FSF and different BSF materials

Table 3. Parameters of GaAs solar cells with InGaP as FSF and different BSF materials

Parameter	*AlGaAs as BSF*	*InGaP as BSF*	*AlGaInP as BSF*
J_{sc} (mA/cm^2)	28.42	28.41	33.35
V_{oc} (V)	1.009	1.008	1.01
P_{max} (mW/cm^2)	24.02	24.09	27.91
FF (%)	83.79	84.08	82.63
η (%)	24.05	24.12	27.94

For further analysis of the reason behind the variation of cell efficiency with varying BSF material, a cross-section of the photogeneration rate and recombination rate is plotted as a function of cell depth as shown in Fig. 7. It can be noticed that the photogeneration and recombination rates for these cells have almost the same trend as for the cells with AlGaAs as the FSF layer described in Fig. 5. The trend variation of the photogeneration and recombination rates of the materials within the BSF layer can be explained using the theory furnished as AlGaAs used as the FSF in subsection 3.2.

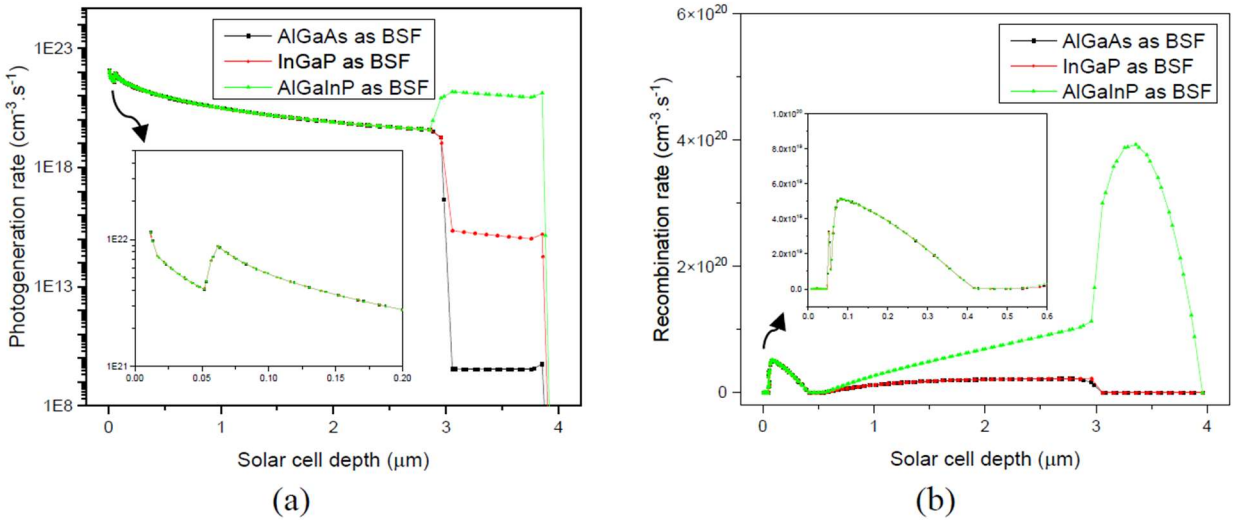

Fig. 7. A cross-section of the (a) photogeneration rate and (b) recombination rate of GaAs solar cells with InGaP as FSF and different BSF materials

3.4 Using AlGaInP as FSF Layer

The resultant J-V characteristics for GaAs solar cells with p-AlGaInP as the FSF layer and n-AlGaAs, n-AlGaInP, and n-InGaP as the BSF layer are illustrated in Fig. 8. Table 4 summarizes the values of the cell's parameters. It can be noted that all cells show almost similar J-V curves and close cell parameter values. The results show that the performance of the cells with AlGaInP as the FSF layer is relatively low, where the conversion efficiency for those cells has an average value of 6.43% which is lower than the efficiency of the initial cell of efficiency 11.42%. Moreover, these cells show relatively low fill factor values which explain the deformation of the squareness in the J-V curves.

To investigate the behavior of the cells with AlGaInP as the FSF layer, a cross-section of the photogeneration and recombination rates along the solar cell is shown in Fig. 9. In Fig. 9(a), the photogeneration rate of these cells shows an optimal value at the top surface of the cells that slowly decreases with the depth of the cells until reaching the BSF layer, then it is suddenly dropped to a further lower value through the BSF layer for the cells with AlGaAs and InGaP as BSF layer, while it is abruptly increased to a new maximum value within the AlGaInP BSF layer. In Fig. 9(b), the recombination within the AlGaInP FSF layer shows a minimal rate, then it abruptly increases to its highest value through the emitter, and then it drops suddenly in the base layer. The recombination rate is dropped further in the BSF layer for the cells with AlGaAs and InGaP as BSF, while it is slightly increased forming a small peak, and decreased again within the AlGaInP BSF. The recombination rate in the AlGaInP BSF layer in this cell is much lower than for the cells with AlGaAs and InGaP as the FSF layer discussed earlier. It is also noticed that the solar cell with AlGaInP BSF shows a relatively stronger recombination rate within both emitter and base layers as compared to the cells with AlGaAs and InGaP as the BSF, which is because of the high photogeneration rate for the cell with AlGaInP as the BSF layer.

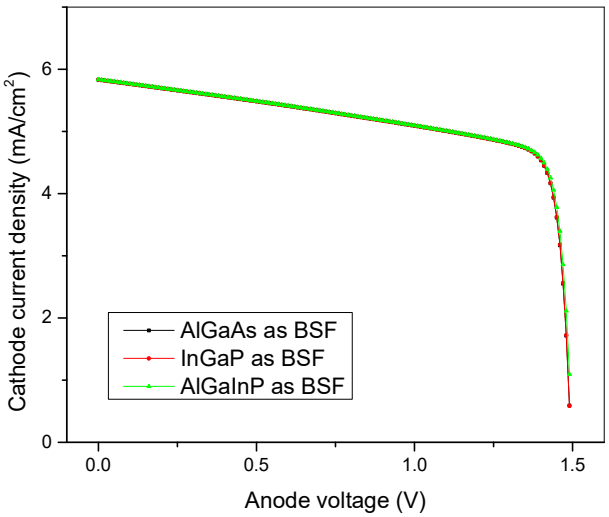

Fig. 8. J-V characteristics for GaAs solar cells with AlGaInP as FSF and different BSF materials

Table 4. Parameters of GaAs solar cells with AlGaInP as FSF and different BSF materials

Parameter	*AlGaAs as BSF*	*InGaP as BSF*	*AlGaInP as BSF*
J_{sc} (mA/cm^2)	5.83	5.83	5.84
V_{oc} (V)	1.49	1.49	1.50
P_{max} (mW/cm^2)	6.14	6.42	6.44
FF (%)	73.61	73.62	73.64
η (%)	6.42	6.42	6.45

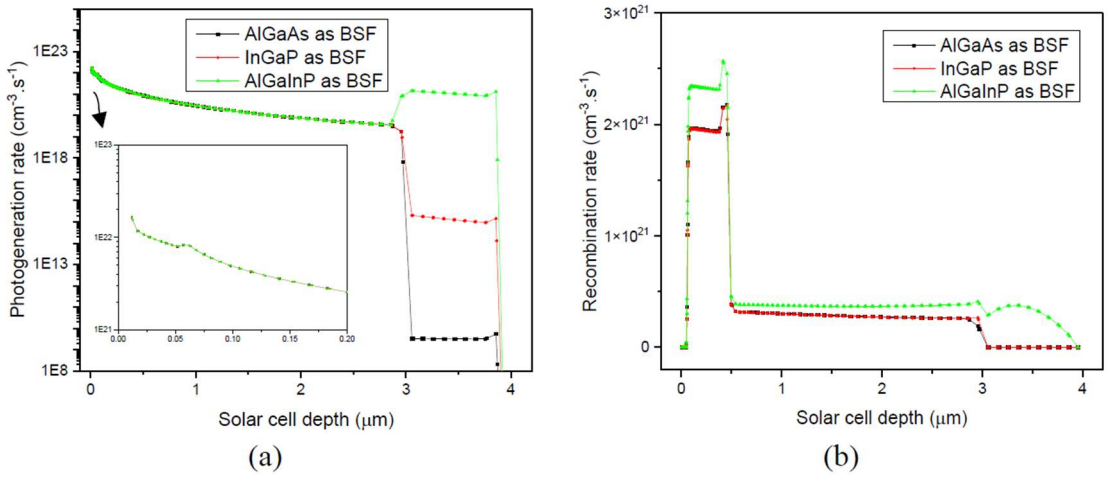

Fig. 9. A cross-section of the (a) photogeneration rate and (b) recombination rate of GaAs solar cells with AlGaInP as FSF and different BSF materials

3.5 Impact of FSF and BSF Energy Band Structure

Fig. 10(a) illustrates the energy-band diagram of solar cells with AlGaAs as the FSF layer and different BSF materials. It can be noticed that the photogenerated electrons in the conduction band of the emitter and base regions are suffering a high energy barrier to escape the cell through the FSF layer, while they are passing easily through the BSF layer and collected at the cathode. While photogenerated holes within the valance band are blocked by the BSF layer energy barrier and pass through the FSF layer to the anode. Furthermore, the relatively high energy bandgap of AlGaInP as a BSF layer offers high confinement for photogenerated carriers within the solar cell, which as a result increases the effectiveness of these carriers to generate higher photocurrent, thus increasing the cell efficiency. Using AlGaInP and InGaP as the FSF layer in the cells shows a similar energy band diagram as for the cells with AlGaAs as the FSF layer, as shown in Fig. 10(b) and 10(c).

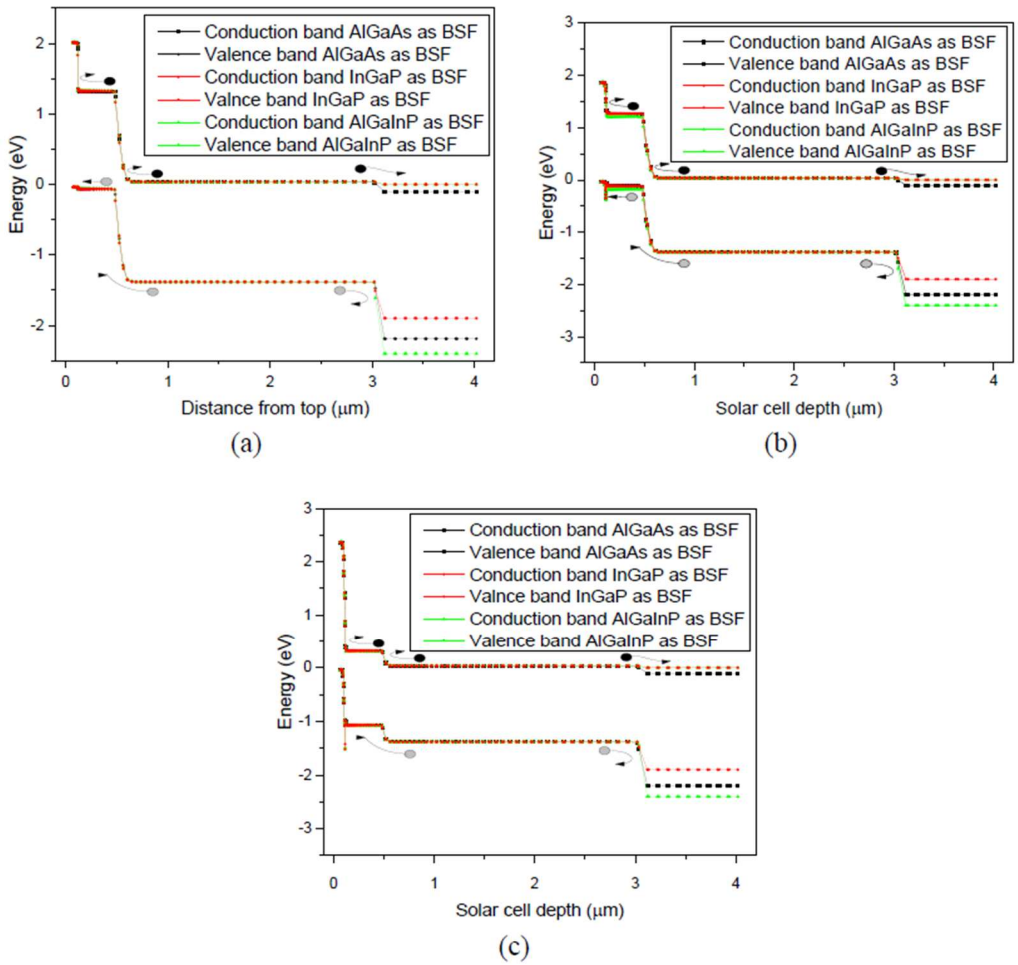

Fig. 10. Energy band diagram of GaAs solar cells with (a) AlGaAs, (b) InGaP, and (c) AlGaInP as FSF and different BSF materials

The impact of the energy band structure of FSF and BSF materials on the attitude of the photogeneration and recombination rates for the suggested cells in this study that directly influence the efficiency is further investigated. The average potential energy difference of the conduction band and valance band between FSF and emitter layers, and between the emitter and base layers, regardless of the BSF material used are evaluated and summarized in Table 5 and Table 6, respectively. The high potential barrier height of the conduction band between FSF and emitter, as well as the low potential step between the emitter and base, in cells with AlGaInP as FSF layer as compared with AlGaAs and InGaP, leads to a higher recombination rate for photogenerated electrons within the emitter (this also explains the high recombination rate within the emitter in figure 9(b)), which resultant with low efficiency for those cells. The high potential barrier in the valance band between the emitter and base layers, when using AlGaAs and InGaP as the FSF, compared to AlGaInP FSF layer, eases the flow of photogenerated holes within the valance band from the base toward the emitter next to the FSF layer and finally to the front contact. Which leads to higher photocurrent and, consequently, higher efficiency.

Table 5. Average energy potential difference for conduction band and valance band between FSF layer and emitter layers

FSF material	Conduction band's potential difference between the FSF and emitter layers	Valance band's potential difference between the FSF and emitter layers
AlGaAs	0.69 eV	0.02 eV
InGaP	0.59 eV	0.08 eV
AlGaInP	2.04 eV	1.03 eV

Table 6. Average energy potential difference for conduction band and valance band between the emitter and base layers

FSF material	Conduction band's potential difference between the emitter and base layers	Valance band's potential difference between the emitter and base layers
AlGaAs	1.28 eV	1.32 eV
InGaP	0.91 eV	1.26 eV
AlGaInP	0.28 eV	0.31 eV

Table 7 displays the potential energy barrier height between the base and BSF layers for both conduction and valance bands at different FSF and BSF materials. It can be noted that the energy differences between the base and BSF of various materials are equal regardless of the FSF material, leading to the conclusion that the impact of the BSF layer on the recombination rate is similar. So, the recombination rate mainly depends on the FSF layer material which controls the potential energy difference between the FSF layer and the emitter region. It can be noticed also that the AlGaInP BSF layer has a relatively low conduction band difference between the base and BSF layers, which allows for photogenerated electrons in the conduction band to flow easily toward the back contact. Furthermore, the AlGaInP BSF layer has the highest valance band difference between the base and BSF layers, which indicates that the maximum number of photogenerated holes in the valance band will be confined in the cell to flow through the FSF layer toward the front contact. Subsequently, this will guarantee high photocurrent to be generated through the cells that are constructed with InGaP and AlGaAs as the FSF layer and AlGaInP as the BSF layer, as a result, high efficiency would be obtained.

Table 7. Potential energy barrier height between the base and BSF layers for both conduction and valance bands at different FSF and BSF material pairs

FSF material	BSF material	Conduction band difference between base and BSF layers	Valance band difference between base and BSF layers
AlGaAs	AlGaAs	0.140 eV	0.81 eV
	InGaP	0.036 eV	0.52 eV
	AlGaInP	0.036 eV	1.02 eV
AlGaInP	AlGaAs	0.140 eV	0.81 eV
	InGaP	0.036 eV	0.52 eV
	AlGaInP	0.036 eV	1.02 eV
InGaP	AlGaAs	0.140 eV	0.81 eV
	InGaP	0.036 eV	0.52 eV
	AlGaInP	0.036 eV	1.02 eV

Out of this research, it can be concluded that the optimum efficiency of GaAs single junction solar cell can be achieved as AlGaAs is used as the FSF layer and AlGaInP is employed as the BSF layer. Additionally, the efficiency of this cell is possibly optimized by controlling the physical parameters of these layers (Saif, 2023; Saif et al., 2023).

4. CONCLUSION

A simulation study for the performance of homojunction GaAs solar cells of different FSF and BSF materials has been carried out using the SILVACO simulator. Where AlGaAs, AlGaInP, and InGaP are used in pairs as FSF and BSF layers. The solar cells are architected with the same doping concentration and thickness for their layers, then their performance is evaluated with the aid of photogeneration rate, recombination rate, and energy band diagram. Based on the results, it is found that:

- The initial cell without FSF and BSF layers records an efficiency of 11.42%. When AlGaAs is utilized as the FSF layer, the efficiency remarkably increases to 25.65%, 30.16%, and 25.72% as AlGaAs, AlGaInP, and InGaP are used for the BSF layer, respectively. When InGaP is served as the FSF layer, the efficiency also increases to 24.05%, 27.94%, and 24.12% as AlGaAs, AlGaInP, and InGaP are used for the BSF layer, respectively. In contrast, once AlGaInP is used as the FSF layer, the efficiency decreases to an average efficiency of 6.43% regardless of the BSF material.
- The high conversion efficiency of the GaAs solar cells that are constructed with AlGaAs and InGaP as the FSF layer is attributed to their high energy bandgap that improves the photogeneration rate and, at the same time guarantees smooth flow for the confined photogenerated electrons toward the back contact.
- The high potential barrier for the valance band between base and BSF when AlGaInP is used as the BSF layer regardless of the FSF material, enhances the ability of confinement for photogenerated holes in the solar cell and smoothens their flow toward the front contact. This makes AlGaInP a highly recommended material to be utilized as a BSF layer in homojunction GaAs solar cells.
- Utilizing AlGaInP as the FSF layer, regardless of the material used for the BSF, maximizes the carriers' recombination within the emitter and base layers, which reduces the number of photogenerated electrons that are

collected by back contact. This makes AlGaInP avoidable material for being used as an FSF layer in GaAs solar cells.

DECLARATION OF COMPETING INTEREST

The authors declare that they have no known competing financial interests or personal relationships that could have appeared to influence the work reported in this paper.

REFERENCES

Abu-Shamleh, A., Alzubi, H., Alajlouni, A. 2021. Optimization of antireflective coatings with nanostructured TiO2 for GaAs solar cells. Photonics and Nanostructures - Fundamentals and Applications, 43, 100862.

Aissat, A., Benyettou, F., Vilcot, J.P. 2017. Electrical and optical properties of InSb/GaAs QDSC for photovoltaic. International Journal of Hydrogen Energy, 42, 19518–19524.

Ansari, Z.A., Singh, T.J., Islam, S.M., Singh, S., Mahala, P., Khan, A., Singh, K.J. 2019. Photovoltaic solar cells based on graphene/gallium arsenide Schottky junction, Optik, 182, 500–506.

Arzbin, H.R., Ghadimi, A., 2019. Improving the performance of a multi-junction solar cell by optimizing BSF, base and emitter layers. Materials Science and Engineering: B, 243, 108–114.

Attari, K., Amhaimar, L., El yaakoubi, A., Asselman, A., Bassou, M. 2017. The Design and Optimization of GaAs Single Solar Cells Using the Genetic Algorithm and Silvaco ATLAS. International Journal of Photoenergy, 2017, 8269358.

Bourbaba, H., Kadri, S., Djermane, K., 2019. Optimization of the performance of GaAs solar cells: Effect of the window layer. Journal of Ovonic Research, 15, 151–156.

Devendra, K.C., Wagle, R., Shrivastava A., Parajuli, D. 2020. InGaP window layer for Gallium Arsenide (GaAs) based Solar Cell using PC1D simulation, Journal of Advanced Research in Dynamical and Control Systems, 12, 2878–2885.

Gamel, M., Jern, K.P., Rashid, E., Jing, L.H., Yao L. K., Wong, B. 2019. Effect of front-surface-field and back-surface-field on the performance of GaAs based-photovoltaic cell. IEEE International Conference on Sensors and Nanotechnology, Penang, Malaysia,1–4.

Islam, M.A., Sulaiman, Y., Amin, N. 2011. A comparative study of BSF layers for ultra-thin CdS:o/CdTe solar cells. Chalcogenide Letters, 8, 65–75.

Kamdem, C.F. Ngoupo, A.T. Konan, F.K. Nkuissi, H.J.T. Hartiti B., Ndjaka, J. 2019. Study of the role of window layer $Al_{0.8}Ga_{0.2}As$ on GaAs-based solar cells performance. Indian Journal of Science and Technology 12, 37, 1–9.

Palacios, C., Guerra, N., Guevara, M., Lopez, M.J. 2018. TCAD 2D numerical simulations for increasing efficiency of AlGaAs – GaAs solar cells. Revista de I+D Tecnológico, 14, 96–107.

Saif, A.A. 2023. High-Efficiency homojunction GaAs solar cell using InGaP as FSF and AlGaInP as BSF. Results in Optics, 12, 100454.

Saif, A.A., Albishri, M., Mindil, A., Qaed, M. 2023. Superior efficiency for homojunction GaAs solar cell. Journal of Ovonic Research, 19, 1–14.

Singh, B., Roshi, Gupta, V. 2022. Impact of different parameters on the performance of GaAs solar cell using PC1D simulation. Materials Today: Proceedings, 62, 6407–6411.

Singh, G., Verma, S.S. 2018. Enhanced efficiency of thin film GaAs solar cells with plasmonic metal nanoparticles. Energy Sources, Part A: Recovery, Utilization, and Environmental Effects, 40, 155–162.

Xu, H., Toprasertpong, K., Delamarre, A., Sodabanlu, H., Watanabe, K., Nakano, Y., Sugiyama, M. 2017. Effect of low-V/III-ratio metalorganic vapor-phase epitaxy on GaAs solar cells. Japanese Journal of Applied Physics, 56, 8S2, 08MC06.

Zhao, Y., Sun, Y., He, Y., Yu, S., Dong, J. 2016. Design and fabrication of six-volt vertically stacked GaAs photovoltaic power converter. Scientific Reports, 6, 38044.